Sufficient conditions for an eigenmanifold to be of the extended Rosenberg type

Cosimo Della Santina (c.dellasantina@tudelft.nl)
TU Delft: Technische Universiteit Delft https://orcid.org/0000-0003-1067-1134
Yannik Wotte
University of Twente: Universiteit Twente
Arne Sachtler
Technical University of Munich: Technische Universitat Munchen
Alin Albu-Scäffer
German Aerospace Center DLR Oberpfaffenhofen Site: Deutsches Zentrum fur Luft- und Raumfahrt DLR Standort Oberpfaffenhofen

Research Article

Keywords: Mechanical Systems , Robotics , Nonlinear Normal Modes , Extended Rosenberg modes

Posted Date: March 9th, 2022

DOI: https://doi.org/10.21203/rs.3.rs-1416735/v1

Nonlinear Dynamics manuscript No.
(will be inserted by the editor)

Sufficient conditions for an eigenmanifold to be of the extended Rosenberg type

Yannik P. Wotte · Arne Sachtler · Alin Albu-Schäffer · Cosimo Della Santina

Received: March 6, 2022/ Accepted: date

Abstract Research in nonlinear modal analysis deals with the extension of linear modes to nonlinear mechanical systems. eigenmanifolds are a recent addition to this field. Pursuing a geometrical viewpoint, they generalize modes to nonlinear mechanical systems with non-constant inertia tensors (e.g., robots, biomechanical models). This work aims at shading light on the connection between this new definition and the well-known extended Rosenberg modes. A key feature of extended Rosenberg modes is that all the associated modal oscillations must intersect at the same point. This appears to be a robust property of oscillations arising when the inertia tensor is constant (Euclidean case). Nevertheless, this symmetry is soon broken when the tensor is configuration-dependent. This paper provides sufficient conditions for this property to be conserved in the non-Euclidean domain, establishing a bridge between the Rosenberg theory and eigenmanifolds. The condition appears to be tight since violating it meant to lose the symmetry in all the tested cases.

Keywords Mechanical Systems · Robotics · Nonlinear Normal Modes · Extended Rosenberg modes

Yannik P. Wotte
Robotics and Mechatronics, University of Twente (UT)
E-mail: y.p.wotte@utwente.nl

Arne Sachtler
Institute of Robotics and Mechatronics, German Aerospace Center (DLR); and Deparment of Informatics, Technical University of Munich (TUM)
E-mail: arne.sachtler@tum.de

Alin Albu-Schäffer
Institute of Robotics and Mechatronics, German Aerospace Center (DLR); and Deparment of Informatics, Technical University of Munich (TUM)
E-mail: alin.albu-schaeffer@dlr.de

Cosimo Della Santina
Institute of Robotics and Mechatronics, German Aerospace Center (DLR); and Cognitive Robotics Department, Delft University of Technology (TU Delft)
E-mail: cosimodellasantina@gmail.com E-mail: c.dellasantina@tudelft.nl

1 Introduction

Linear modes are a powerful tool for studying and characterizing families of regular oscillations that consistently arise in linear mechanical systems. Eigenspaces are the bi-dimensional and flat collections of these orbits. The quest for a reliable generalization of this concept to the nonlinear case keep scientists busy since the times of Poincaré and Lyapunov. A survey of these efforts is provided in [3]. Among existing definitions Rosenberg [1] and extended Rosenberg modes [2] had probably the larger impact in the literature (see Figs. 1a and 1b, respectively). Both types of modes are defined as line-shaped evolutions in configuration space that pass through the equilibrium configuration. Rosenberg modes have the further restriction that all joints' coordinates must oscillate in unison.

A main limitation of (extended) Rosenberg modes (ERMs) is that they are not applicable to systems with non constant inertia tensor - i.e. having configuration space equipped with non-Euclidean metric. This is connected to how they have historically evolved, but most importantly because oscillations in these systems rarely pass through the equilibrium. This in turn makes it nontrivial to distinguish isolated oscillations from modes. This is discussed in detail in [3, Sec. 7.1]. Note that non-Euclidean cases are far from being corner examples, since they include many mechanical structures with clear practical relevance in science and engineering

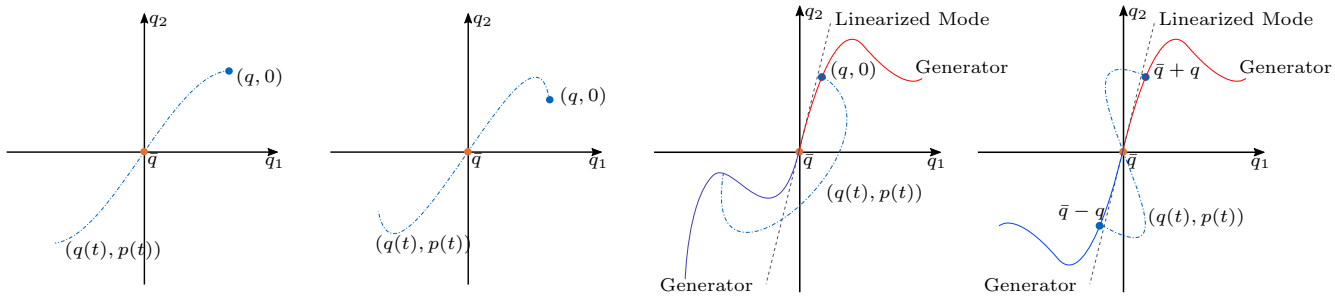

(a) Rosenberg Mode (b) Extended Rosenberg Mode (c) Eigenmanifold Generators (d) Generator on ERM.

Fig. 1: Types of nonlinear normal modes in conservative systems. W.l.o.g. the equilibrium $\bar{q}$ is assumed to be located at the origin. **(a)** Rosenberg modes: all coordinates oscillate in unison and pass through the equilibrium configuration [1]. **(b)** Extended Rosenberg modes: a relaxation of Rosenberg modes that does not require coordinates to oscillate in unison [2]. **(c)** The definition of Eigenmanifolds as collections of initial positions of line-shaped modes, where the collection of initial conditions originates in the equilibrium [3]. **(d)** This paper presents that under certain conditions on the mass-matrix and the potential, all modes collected on Eigenmanifolds are guaranteed to be extended Rosenberg modes.

- as for example robots [4,5] and models in biomechanics, like an animal body [6,7]. Fig. 2 shows two simple examples of Euclidean and non-Euclidean mechanical systems.

Eigenmanifolds have been recently proposed in [3] as a way of overcoming this limitation. The key idea is to look for a direct geometrical generalization of the flat eigenspaces to a curved counterpart in the non-Euclidean domain. These are 2-dimensional manifolds embedded within the state-space of mechanical systems, containing a unique equilibrium and collecting trajectories that are periodic, and line-shaped in configuration space (see Fig. 1c). This definition has shown to be selective enough to consistently give n solutions for configuration spaces of dimension n, but at the same time general enough to be applicable to mechanical systems with non constant inertia tensor. Note however that a formal proof of the former statement is still to be provided.

The introduction of this new general definition opens up the question: how are eigenmanifolds connected with classic Rosenberg theory? We aim here at making a substantial step towards clarifying this connection. More specifically, we prove that if the potential field and the inertia tensor are simultaneously even-symmetric in some choice of coordinates, then the eigenmanifold will be of the extended Rosenberg type.

The rest of the paper is organized as follows. First, a brief state of the art concludes this introductory section. Then, in Sec. 2 we briefly introduce some notation from Hamiltonian mechanics, and we re-formulate the main definitions from eigenmanifold theory in this formalism. Note indeed that [3] uses Lagrangian formalism. This different formulation is instrumental to deriving two simple symmetries in Sec. 3, where some of their implications for periodic solutions on eigenmanifolds are also highlighted. These preliminary results are leveraged in Sec. 4 where the main theoretical contribution of this paper is derived and discussed. Afterwards, in Sec. 5, we show concrete example systems satisfying and violating the conditions required to be of extended Rosenberg type. These examples should provide a visual understanding of the structure behind nonlinear normal modes. Finally, Sec. 6 draws the conclusions of this work.

1.1 Related Literature

Nonlinear normal modes (NNMs) of conservative mechanical systems are reviewed in [3], which identifies Rosenberg modes [1] and extended Rosenberg modes [2] as commonly used types of nonlinear modes in the numerical analysis of conservative mechanical systems with a constant inertia tensor. Renson et al. review numerical techniques for the computation of nonlinear modes [8], and Ehrhardt et al. give an example of their experimental application to a cross-beam structure and the interaction of torsional NNMs with bending NNMs [9]. Avramov et al. [10] refer to various applications, both of Rosenberg modes to conservative mechanical systems and of Shaw-Pierre modes [11] to damped mechanical systems. Mixed analytic and numeric examples of analyzing nonlinear normal modes are given for a nonlinear two mass system by Vakakis et al. [12] and for a double pendulum (prior to the differential geometric definition of eigenmanifolds) by Kovacic et al. [13].

From a technological application standpoint, eigenmanifold stabilization [14,15,16] has proven to be a robust and effective way of exciting efficient nonlinear oscillations - which is an open challenge in nonlinear

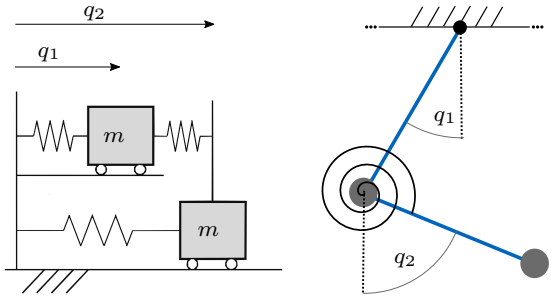

(a) Euclidean system (b) Non-Euclidean system

Fig. 2: Examples of two simple mechanical systems systems with different inertia properties. The one in Panel (a) is obtained by interconnecting two masses moving on linear rails with possibly nonlinear springs. This system has an inertia which is independent on the configuration. The natural metrics of the configuration space is therefore Euclidean. Panel (b) reports a double pendulum with a spring connected in parallel to the second joint. This system has configuration dependent inertia, since the inertia seen by the first joint depends on the angle assumed by the second joint. As a consequence the configuration space is curved and is equipped with a non-Euclidean metrics. Note that in case of linear springs the former can be seen as a linear approximation of the latter.

control theory [17,18,19], robotics [20,21,22,23], and biomechanics [24,25,26].

A general treatment of symmetries in dynamical systems is given by Baake [27]. Symmetries of Hamiltonian systems are typically the focus of studies in the context of conserved quantities arising through Noether's theorem [28,29,30,31]. Large classes of these symmetries were also studied in the context of periodic orbits and nonlinear normal modes [32,33]. Within the nonlinear modes literature, possibly the most relevant use of symmetries is by Rosenberg [1]. In his seminal work, he defines admissible systems via an assumption of symmetry, for which fundamental properties of Rosenberg modes are consequently derived. The effect of symmetries on stability of dynamic systems was discussed in the context of control by Russo et al. [34], while Ozana et al. [35] used the concept of time-reversiblity for trajectory planning in nonlinear mechanical systems.

2 Background

2.1 System Definition

This work deals with nonlinear mechanical system not subject to holonomic constraints. We provide in this section a short summary of the notation of the geometrical view to classic mechanics. The interested reader can refer to [36] for a comprehensive introduction on the topic.

The configuration space of a mechanical system can be modeled by a Riemannian manifold $(\mathfrak{X},\ g)$ of dimension n, with metric tensor g. Here, $x \in \mathfrak{X}$ denotes a generic point on $\mathfrak{X}$. The corresponding system velocity v at x is then an element of the tangent space $v \in T_x\mathfrak{X}$, while the momentum exists in the cotangent space $T_x^*\mathfrak{X}$. Evolutions of the system are geodesics on $\mathfrak{X}$ with respect to the Jacobi metric. The natural choice for g is the kinetic energy of the system. This metric is a standard Euclidean one if the system's inertia is not configuration dependent (Fig. 2a). This in turn implies that the curvature of $\mathfrak{X}$ is null everywhere. If instead the mechanical system is not a discrete set of masses interconnected through a potential field (see for example the double pendulum in Fig. 2b) then the metric g is not Euclidean and the configuration space is curved.

Working directly in coordinate free notation is often unpractical. Therefore, we suppose that a large enough chart $\mathfrak{X}$ is available, which also includes at least one equilibrium of the system. Under this chart, the coordinates of configuration variables are $q \in \mathbb{R}^n$, the momentum variables are $p = M(q)\dot{q} \in \mathbb{R}^n$ and the symmetric, positive-definite mass-matrix is $M(q) \in \mathbb{R}^{n\times n}$. They respectively follow from the configuration x, velocity v, momentum and inertia tensor of the coordinate free system, while the potential function $V(q)$ also stems from a coordinate-free analog.

The dynamics of these systems can be written in Hamiltonian form (see [37] for more details)

$$\dot{q} = \frac{\partial H}{\partial p}(q,p), \qquad \dot{p} = -\frac{\partial H}{\partial q}(q,p), \tag{1}$$

where the Hamiltonian $H(q,p)$ is given by

$$H(q,p) = \frac{1}{2}p^T M(q)^{-1} p + V(q). \tag{2}$$

We will refer to a tuple of q and p, thus an element of the state space, as $z = (q,p)$ and for trajectories we will write $z(t) = (q(t), p(t))$.

2.2 Definition of Nonlinear Modes and Eigenmanifolds

An in-detail introduction to Eigenmanifolds is provided in [3, Sec. 7]. We provide here a short summary of the most important concepts.

The definition of Eigenmanifolds relies on the concept of the generator, a collection of points $(x, 0)$ in the tangent bundle $T\mathfrak{X}$, starting at an equilibrium $(x_{\text{eq}}, 0)$ [3]. With $T\mathcal{U} \subset T\mathfrak{X}$ being a generic subset of the state space, let $\mathrm{G}(T\mathcal{U})$ return the collection of forward and backward orbits originating from each point in $T\mathcal{U}$. Then the generator is defined as follows:

Definition 1 (Generator) Consider a 1-dimensional connected submanifold $\mathcal{R} \subseteq T\mathfrak{X}$. We call it a generator for $\mathfrak{M}$ if

i $\mathfrak{M} = \mathrm{G}(\mathcal{R})$ is a 2-dimensional (invariant) manifold,
ii $\forall (x, v) \in \mathcal{R}$ it holds $v = 0$,
iii $\exists! (x_{\mathrm{eq}}, 0) \in \partial\mathcal{R}$ such that $\{(x_{\mathrm{eq}}, 0)\}$ is invariant - i.e. it is an equilibrium.

Then the definition of eigenmanifolds follows by demanding a generator to be found for a collection of particular periodic orbits:

Definition 2 (Eigenmanifold) A 2-dimensional invariant sub-manifold $\mathfrak{M} \subseteq T\mathfrak{X}$ admitting a generator is an eigenmanifold if

i Trajectories within $\mathfrak{M}$ are periodic,
ii Trajectories within $\mathfrak{M}$ are line-shaped when projected to $\mathfrak{X}$.

Based on continuity arguments of the flow f and unicity of solutions, only two generators $\mathcal{R}$ are associated to a given eigenmanifold. Based on similar arguments, we assume $\mathcal{R}$ and $\mathfrak{M}$ to be smooth.

The objects in these definitions can be rewritten into coordinates by employing charts $\Phi : \mathcal{U} \subset \mathfrak{X} \to \mathbb{R}^n$ and $\mathrm{d}\Phi_x : T_x\mathfrak{X} \to \mathbb{R}^n$ mapping $(x, v) \to (q, \dot{q})$ [3], with q and $\dot{q}$ as above. In the following, a single global chart is assumed to chart all points (x, v) to (q, p) and generators are denoted as 1-dimensional manifolds $\mathcal{R} \subset \mathbb{R}^{2n}$, while eigenmanifolds are 2-dimensional manifolds $\mathcal{M} \subseteq \mathbb{R}^{2n}$. Note that charting $(x, v) \in T\mathfrak{X}$ to configuration q and momentum p turns the generators from curves on $T\mathfrak{X}$ into curves on $T^*\mathcal{M}$, which is a well-defined transformation via the inertia tensor of any given system.

Remark 1 Note that the results presented in the following hold, as long as a chart of $\mathfrak{X}$ exists such that the given conditions can be guaranteed. We prefer to keep the derivation in coordinates for the sake of readability. For a differential geometric view, refer to the appendix.

2.3 Extended Rosenberg Eigenmanifolds

In this context, we can easily further extend Rosenberg definition to the non-Euclidean domain as follows [3, Sec. 7.5]:

Definition 3 (Extended Rosenberg Mode) An Eigenmanifold is of the Extended Rosenberg kind if all trajectories contained in it are Extended Rosenberg Modes - i.e. they pass through the equilibrium configuration x_{eq} when projected to $\mathfrak{X}$.

The research question that we aim to answer with this work can now be clearly formulated as: *under conditions an Eigenmanifold $\mathfrak{M}$ is a Rosenberg manifold?*

3 Symmetries within Conservative Mechanical Systems

We introduce here two symmetries of Hamiltonian systems. The first one holds in general, and as such is well known in the literature. For convenience, we report two Lemmas based on it. The second symmetry is specific for systems with Hamiltonian as in (2), and it holds only for certain choices of M and V. We then prove two simple Lemmas that will be later instrumental to the proof of the main Theorem.

3.1 Time Reversal Symmetry

The equations of motion verify the following well known symmetry [38]

$$(q, p, t) \to (q, -p, -t). \tag{3}$$

In other words, if an evolution $(q(t), p(t))$ is a solution of (1), then so is $(q(-t), -p(-t))$. The following Lemma holds thanks to this symmetry.

Leveraging this symmetry, we prove two properties of trajectories that start at $p(0) = 0$, which we present below and we apply later to modal evolutions.

Lemma 1 *Consider an evolution $(q(t), p(t)) : \mathbb{R} \to \mathbb{R}^{2n}$. If there are two instants $t', t'' \in \mathbb{R}$ such that $p(t') = p(t'') = 0$, then the evolution is periodic with period $T = 2|t'' - t'|$.*

Proof Without loss of generality, assume $t'' > t'$ and denote $\Delta t = t'' - t'$. By (3), if an evolution $z_1(t) = (q(t' + t), p(t' + t))$ satisfies (1), then there is a corresponding evolution $z_2(t) = (q(t' - t), -p(t' - t))$ that likewise satisfies (1). By assumption it holds that $p(t') = p(t'') = 0$, so

$$z_1(0) = (q(t'), 0)\,, \tag{4}$$
$$z_1(\Delta t) = (q(t''), 0)\,. \tag{5}$$

The corresponding solution $z_2(t) = (q(t' - t), -p(t' - t))$ satisfies

$$z_2(0) = (q(t'), 0)\,, \tag{6}$$
$$z_2(-\Delta t) = (q(t''), 0)\,. \tag{7}$$

Since the solutions of (1) are unique, it follows from $z_1(\Delta t) = z_2(-\Delta t)$ that $z_1(\Delta t + t) = z_2(-\Delta t + t)$. Subsequently choose $t = \Delta t$ to find $z_1(2\Delta t) = z_2(0) = z_1(0)$. □

Lemma 2 *Given $T > 0$, a T-periodic orbit $(q(t), p(t))$ with $(q(t), p(t)) = (q(t + T), p(t + T))$ encounters either 0 or 2 distinct points with $p(t) = 0$.*

Proof (Lemma 2) Let one point with $p(t') = 0$ be encountered by a T-periodic orbit $(q(t), p(t))$, and note that both $z_1(t) = (q(t'+t), p(t'+t))$ and $z_2(t) = (q(t'-t), -p(t'-t))$ are valid periodic solutions, with $z_2(t)$ following via (3). Since $p(t') = 0$, it holds that $z_1(0) = z_2(0)$. From uniqueness of solutions it then follows that $z_1(t) = z_2(t)$ for any t, so also that $z_1(T/2) = z_2(T/2)$:

$$p(t' + T/2) = -p(t' - T/2)\,. \tag{8}$$

By periodicity, $z_1(T/2) = z_1(-T/2)$:

$$p(t' + T/2)) = p(t' - T/2))\,. \tag{9}$$

Substituting (8) into (9) shows

$$-p(t' - T/2) = p(t' - T/2)\,, \tag{10}$$

from which follows that $p(t' - T/2) = 0$. Thus, any periodic solution that encounters a point with zero momentum once, also encounters a distinct second point with zero momentum.

Even more, since $z_1(t) = z_2(t)$ then the evolution of

$$q(t' + t) = q(t' - t), \tag{11}$$

Thus, the evolutions in configuration space between two points with zero momentum coincides. Encountering more than two points with zero momentum is therefor not possible. Indeed, if this happened then (11) would apply and assure that the trajectory is followed back to $q(t')$ - therefore preventing the reaching of $q(t' + T/2)$.

The only alternative left are trajectories that encounter $p(t) = 0$ times, like the circular motion with constant velocity of a particle.

□

Corollary 1 *To each eigenmanifold $\mathfrak{M}$ are associated exactly two generators $\mathcal{R}$.*

Proof The Corollary directly follows from Lemma 2 by considering that a generator is defined as the collection of the states with zero momentum across modal oscillations, and that the modes are line-shaped by definition - thus implying that there are two points of zero velocity. □

3.2 Equivariant Symmetry

Given a trajectory $q(t) = \bar{q} + \hat{q}(t)$ with $\bar{q}$ constant, (1) is invariant under a change of coordinates

$$(\bar{q} + \hat{q}, p, t) \to (\bar{q} - \hat{q}, -p, t) \tag{12}$$

as long as $H(\bar{q} + \hat{q}, p) = H(\bar{q} - \hat{q}, p)$, and $H(q, p) = H(q, -p)$. Note that compared to (3) we are not inverting here the direction of the time arrow.

The latter condition is trivially satisfied for a mechanical system, since $H(q, p)$ is quadratic in p, see (2). The first condition is fulfilled if and only if the inertia matrix and the potential field are simultaneously even symmetric about $\bar{q}$, i.e.,

$$M(\bar{q} + \hat{q}) = M(\bar{q} - \hat{q}) \tag{13}$$

and

$$V(\bar{q} + \hat{q}) = V(\bar{q} - \hat{q}). \tag{14}$$

Symmetry (12) leads to two properties of periodic trajectories within the system (1), which are collected in Lemma 3 and Lemma 4. As such, these Lemmas also hold for modes collected on eigenmanifolds.

Lemma 3 *If two points $z(0) = (\bar{q} + \hat{q}(0), p(0))$ and $z(t') = (\bar{q} - \hat{q}(0), -p(0))$ lie on the same $T-$periodic orbit, then it holds for all t that*

$$\begin{cases} \hat{q}(t + T/2) = -\hat{q}(t) \\ p(t + T/2) = -p(t)\,. \end{cases} \tag{15}$$

Proof (Lemma 3) Let $z_1(t) = (\bar{q} + \hat{q}(t), p(t))$ be a solution to the equations of motion (1). Via (12), a $z_2(t) = (\bar{q} - \hat{q}(t), -p(t))$ must also be a solution. Since $z_1(0) = (\bar{q} + \hat{q}, p)$ and $z_2(0) = (\bar{q} - \hat{q}, -p)$, then by hypothesis

$$z_1(t') = z_2(0)\,. \tag{16}$$

Thus $\hat{q}(t') = -\hat{q}(0)$ and $p(t') = -p(0)$ can be substituted into $z_2(t)$ to find $z_2(t') = z_1(0)$. Thus $t' = T/2$, and (16) can be re-formulated as $z_1(T/2) = z_2(0)$. Evaluating the forward evolution of both trajectories yields $z_1(t + T/2) = z_2(t)$, which is (15). □

Lemma 4 *If two points $z(t') = (\bar{q} + \hat{q}, 0)$ and $z(t'') = (\bar{q} - \hat{q}, 0)$ lie on the same T-periodic orbit, then $\nu \in \mathbb{R}^n$ exists such that $z(t' + T/4) = (\bar{q}, \nu)$.*

Proof (Lemma 4) Thanks to Lemma 1 we can say that $t'' = t' + T/2$. Then, following the same reasoning of the proof of Lemma 2, we can get to (11) and evaluate it at time $T/4$. This yields $q(T/4) = q(-T/4)$, and hence

$$\hat{q}(T/4) = \hat{q}(-T/4)\,. \tag{17}$$

We can now use Lemma 3, for the case in which the momentum of the two states is zero. This allows substituting $t = -T/4$ in (15), which results in

$$\hat{q}(T/4) = -\hat{q}(-T/4)\,. \tag{18}$$

Combining (17) and (18) yields $\hat{q}(-T/4) = -\hat{q}(-T/4)$, which implies

$$\hat{q}(T/4) = 0\,, \tag{19}$$

from which it follows that $q(T/4) = \bar{q}$. □

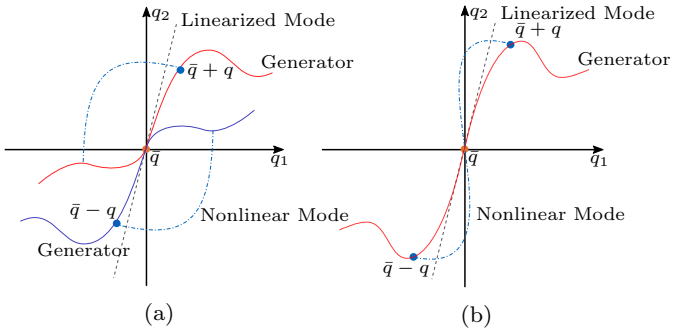

Fig. 3: A motivation of condition ii) in Theorem 1. **a)** This scenario is possible when condition ii) is not given, since for any mode $(\bar{q}+\hat{q}(t), p(t))$ only a symmetric mode $(\bar{q}-\hat{q}(t), -p(t))$ is guaranteed. **b)** If the generator is unique, however, then the modes $(\bar{q}+\hat{q}(t), p(t))$ and $(\bar{q}-\hat{q}(t), -p(t))$ must trace the same evolution.

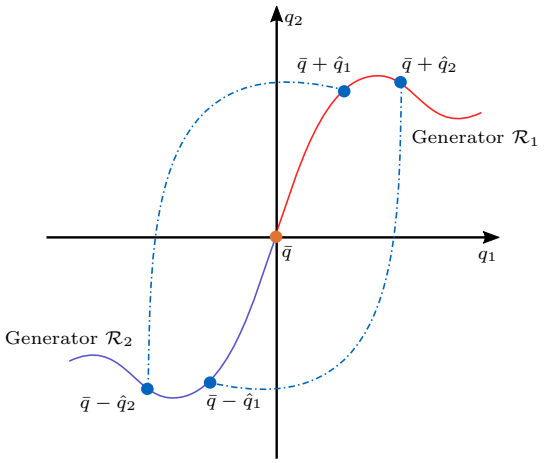

Fig. 4: Scenario that we want to make sure it is not possible in the (a) part of the proof of Theorem 1.

4 Sufficient condition for extended Rosenberg modes

This section introduces the main result of this paper, combining the symmetries introduced in Sec. 3 with modal theory.

Theorem 1 (Existence of ERM families) *Consider an eigenmanifold $\mathfrak{M}$ of the system (1) with generator $\mathcal{R}$, and containing the equilibrium $\bar{q}$.*

Then $\mathfrak{M}$ is an extended Rosenberg eigenmanifold if the following two conditions hold simultaneously

- *i* ***Even-symmetry:*** *$\forall \hat{q}$, $V(\bar{q}+\hat{q}) = V(\bar{q}-\hat{q})$ and $M(\bar{q}+\hat{q}) = M(\bar{q}-\hat{q})$;*
- *ii* ***Unicity:*** *$\nexists \mathcal{R}'$ s.t. $T_{(\bar{q},0)}\mathcal{R}' = T_{(\bar{q},0)}\mathcal{R}$, and $G(\mathcal{R}') \neq \mathfrak{M}$, where $G(\mathcal{R}')$ is an eigenmanifold of (1).*

Fig. 3 visualizes the idea behind ii: this condition is required to prove that for a mode starting at $(\bar{q}+\hat{q}_0, 0)$, also $(\bar{q}-\hat{q}_0, 0)$ lies on the same mode, from which it directly follows via Lemma 4 that such a mode is an extended Rosenberg mode.

Proof (Theorem 1) Thanks to Corollary 1 we can say that there are only two different generators associated to the eigenmanifold. For the sake of clarity, we refer to $\mathcal{R}$ as $\mathcal{R}_1$, and to the other generator of $\mathfrak{M}$ as $\mathcal{R}_2$. Condition (i) allows to apply symmetry (12) to the system (1). In other words, if $(\bar{q}+\hat{q}(t), p(t))$ is an evolution of the system, then $(\bar{q}-\hat{q}(t), -p(t))$ is also a solution of the system.

Taken an initial condition $(\bar{q}+\hat{q}(0), 0) \in \mathcal{R}_1$, then the associated evolution $(\bar{q}+\hat{q}(t), p(t))$ by definition. Thus, thanks to the symmetry, $(\bar{q}-\hat{q}(t), -p(t))$ has the same characteristics of the initial evolution, i.e. it is periodic and line-shaped. This can be repeated for all points in $\mathcal{R}_1$, starting form the equilibrium. Therefore, the collection of the points $(\bar{q}-\hat{q}(0), 0)$ so obtained identified a generator generator $\mathcal{R}'$. Then, $\mathfrak{M}' = G(\mathcal{R}')$ is an eigenmanifold of (1). Note that $\mathcal{R}' \neq \mathcal{R}_1$ by construction, however it is not necessarily the case that $\mathcal{R}' = \mathcal{R}_2$ (see Fig. 3a). If $\mathcal{R}' \neq \mathcal{R}_2$ then $\mathfrak{M}' \neq \mathfrak{M}$.

Consider the two parametrized smooth curves

$$\gamma_{\mathcal{R}_1} : \mathbb{R}^+ \to \mathcal{R}_1, \quad \gamma_{\mathcal{R}'} : \mathbb{R}^+ \to \mathcal{R}', \tag{20}$$

defined such that for all $s \in \mathbb{R}^+$ then there exists a $\hat{q} \in \mathbb{R}^n$ such that

$$\gamma_{\mathcal{R}_1}(s) = (\bar{q}+\hat{q}(s), 0) \qquad \gamma_{\mathcal{R}'}(s) = (\bar{q}-\hat{q}(s), 0). \tag{21}$$

This is always possible because of how $\mathcal{R}_1$ and $\mathcal{R}'$ are defined. Also, without loss of generality we take $\gamma_{\mathcal{R}_1}(0) = (\bar{q}, 0)$, which implies $\gamma_{\mathcal{R}'}(0) = (\bar{q}, 0)$. Then the tangent vector to $\mathcal{R}_1$ at $(\bar{q}, 0)$ is $\frac{\partial \gamma_{\mathcal{R}_1}}{\partial s}(0) = (\frac{\partial \hat{q}}{\partial s}(0), 0) = -\frac{\partial \gamma_{\mathcal{R}'}}{\partial s}(0)$. Thus, the two generators are tangent to a same vector at the equilibrium, and therefore $T_{(\bar{q},0)}\mathcal{R}' = T_{(\bar{q},0)}\mathcal{R}_1$. But the existence of such an $\mathcal{R}'$ is excluded by hypothesis (ii). Thus $\mathcal{R}' = \mathcal{R}_2$, which means that we are in the condition described by Fig. 3b.

What is therefore left to prove is that if the two generators are symmetric, then all the associated modal evolutions pass through the equilibrium configuration. This can be shown in two steps:

(a) proving that two points $(\bar{q}+\hat{q}, 0)$ and $(\bar{q}-\hat{q}, 0)$ always lie on the same mode;
(b) showing that (a) yields the mode passing via $\bar{q}$.

However, point (b) is implied by direct application of Lemma 4. Thus, proving (a) will conclude the proof. Note that this will be equivalent to proving that the scenario in Fig. 4 is impossible. We start by defining the map

$$f : \mathcal{R}_1 \to \mathcal{R}_2, \tag{22}$$

associating each end of the mode to the other end - i.e., such that $f(z_1) = z_2$. The inverse f^{-1} is therefore such that $f^{-1}(z_2) = z_1$. Smoothness of the generators guarantees that f and f^{-1} are continuous.

Then define $F : \mathbb{R}^+ \to \mathbb{R}^+$ as f expressed in chart coordinates

$$F(s) = \Sigma_{\mathcal{R}_2}(f(\Sigma_{\mathcal{R}_1}^{-1}(s))), \tag{23}$$

where we introduce the global charts[1]

$$\Sigma_{\mathcal{R}_1} : \mathcal{R}_1 \to \mathbb{R}^+, \quad \Sigma_{\mathcal{R}_2} : \mathcal{R}_2 \to \mathbb{R}^+, \tag{24}$$

such that $\Sigma_{\mathcal{R}_1}((\bar{q} + \hat{q}, 0)) = \Sigma_{\mathcal{R}_2}((\bar{q} - \hat{q}, 0))$. Furthermore, without loss of generality, let $\Sigma_{\mathcal{R}_1}((\bar{q}, 0)) = 0$ and $\Sigma_{\mathcal{R}_2}((\bar{q}, 0)) = 0$. Thus, proving (a) is equivalent to proving that F is the identity function.

Due to the symmetry discussed at the very beginning of the proof, It is also the case that

$$F(s) = \Sigma_{\mathcal{R}_1}(f^{-1}(\Sigma_{\mathcal{R}_2}^{-1}(s))). \tag{25}$$

This map satisfies $F(0) = 0$, since the equilibrium $(\bar{q}, 0)$ is a fixed point and $\Sigma_{\mathcal{R}_1}((\bar{q}, 0)) = \Sigma_{\mathcal{R}_2}((\bar{q}, 0)) = 0$.

Combining (23) and (25) yields

$$F(F(s)) = s. \tag{26}$$

In general, equation (26) has an uncountable number of continuous solutions. However, with the constraints that $F(0) = 0$ and $F(s) \geq 0$, the only admissible solution is

$$F(s) = s. \tag{27}$$

Thus F is the identity function, which proves point (a) thus concluding the proof.

□

5 Examples

This section presents two examples. The first one highlights the various aspects of Theorem 1. This is done with two low dimensional systems to ease visual understanding. The second one is higher dimensional, which shows that the proposed result holds for non trivial systems.

[1] They can be thought of as a generalized energy.

5.1 Extensive analysis of 2-DoF systems

We consider a Euclidean system having a metric tensor of the form $M = mI$ and a non-Euclidean system on curved configuration space. The first is shown in Fig. 2a, and the latter is the double pendulum with parallel elasticity shown in Fig. 2b. We also consider multiple choices of potential functions. We achieve a variety of systems, some of which will satisfy the conditions of Theorem 1 and some will not. This way, we can observe the implication of Theorem 1 to the model oscillations of the potentially non-linear system.

Denote the constant inertia of a linear two-mass system as

$$M_C(q) = \begin{bmatrix} m & 0 \\ 0 & m \end{bmatrix}. \tag{28}$$

Also, we denote the inertia of the double-pendulum by

$$M_{DP}(q) = \begin{bmatrix} m_{11} & m_{12} \\ m_{12} & m_{22} \end{bmatrix}, \tag{29}$$

where

$$m_{11} = I + 3d^2m + 2d^2m\cos(q_2) \tag{30}$$
$$m_{12} = d^2m(1 + \cos(q_2)) \tag{31}$$
$$m_{22} = I + d^2m. \tag{32}$$

We introduce the following choices of potential functions

$$V_a(q) = {}^1\!/_2 k(q_2 - {}^\pi\!/_2)^2 - dmg(2\cos(q_1) + \cos(q_1 + q_2)),$$
$$V_{s1}(q) = {}^1\!/_2 k(q_2)^2 - dmg(2\cos(q_1) + \cos(q_1 + q_2)),$$
$$V_{s2}(q) = {}^1\!/_2 k q_1^2 + {}^1\!/_2 k(q_2 - {}^\pi\!/_2)^2.$$

Note that the first function is asymmetric and the latter two are symmetric. Parameters are chosen as summarized in Tab. 1. We combine the metric tensors and the potential functions in order to obtain a variety of systems. In all combinations the dynamics are governed by (1). The results from numerical continuation are summarized in Figs. 5, 6 and in Tab. 2. The case of (M_C, V_{s2}) is omitted since it is a linear system and thus of little interest.

Table 1: Parameters for the example systems

Parameter	Value
m	0.4 kg
I	$^1/_{12}$ kgm^2
d	1 m
k	10 Nm/rad
g	9.81 m/s^2

Table 2: Summary of tested 2−DoF examples

System	System type	Potential	In. tensor	Theorem 1 Satisfied?	Figure
(M_{DP}, V_{s1})	non-Euclidean	Symmetric	Symmetric	✓	Fig. 5a, 5b
(M_{DP}, V_a)	non-Euclidean	Asymmetric	Symmetric	✗	Fig. 5c, 5d
(M_{DP}, V_{s2})	non-Euclidean	Symmetric	Asymmetric	✗	Fig. 5e, 5f
(M_C, V_{s1})	Euclidean	Symmetric	Symmetric	✓	Fig. 5g, 5h
(M_C, V_a)	Euclidean	Asymmetric	Symmetric	✗	Fig. 5i, 5j

As expected via Theorem 1, the symmetric double pendulum with gravity and a spring at the second joint (M_{DP}, V_{s1}) shows families of extended Rosenberg modes collected on the generators. Example modes on its generators are shown in Fig. 5a & 5b.

When the equilibrium of the spring is changed to $\pi/2$ by choosing (M_{DP}, V_a), the families of nonlinear oscillations cease to consist exclusively of extended Rosenberg modes. This is shown in Fig. 5c & 5d. As an additional example of the conditions of Theorem 1 not being satisfied, note that continuous families of extended Rosenberg modes are also not present in the case of (M_{DP}, V_{s2}), i.e., for a double pendulum with only a spring at the second joint. In this case, the inertia tensor is not symmetric w.r.t. the equilibrium configuration, since the latter is not the straight configuration. This is shown in Fig. 5e & 5f. In the case of a constant mass-matrix M_C, families of extended Rosenberg modes are indeed found if the symmetric potential V_{s1} (or trivially V_{s2}) is used. This is shown for the case of V_{s1} in Fig. 5g & 5h. More surprisingly, the violation of Theorem 1 by using the asymmetric potential V_a also leads to the disappearance of continuous families of extended Rosenberg modes for this constant mass-matrix. This is shown in Fig. 5i & 5j. Therefore, the extended Rosenberg definition appears to be not general enough to represent all systems with Euclidean metrics.

Lastly, although we provide only a sufficient condition, we could not find any example of Rosenberg's manifolds for systems not fulfilling the hypotheses of Theorem 1. However, we observe that it is not uncommon to find isolated extended Rosenberg modes which are not excluded by Theorem 1. This is highlighted by Fig. 6, which shows the minimum potential energy V along a given mode together with the energy of the starting point of that mode for all five systems. Whenever this minimum potential is zero, it means that the corresponding mode passes through the equilibrium. Thus, isolated zeros of this function identify isolated extended Rosenberg modes within non-Rosenberg eigenmanifolds.

5.2 Example of high dimensional system

Let us now analyze the nonlinear normal modes of a more complex system satisfying the symmetry conditions required by Theorem 1. We take a quintuple pendulum as shown in Fig. 7 and set all masses to $m = 0.4\text{Kg}$ and the link lengths $l = 1.0\text{m}$. Further we use a diagonal stiffness matrix $K = 20I\frac{\text{Nm}}{\text{rad}}$ and set $g = -9.81\frac{m}{s^2}$. Our aim is showing that this rather complicated system satisfies the theorem and that we can observe the predicted result, i.e., all modal oscillations passing through the equilibrium.

Concerning the choice of the potential field, consider that in the case that the equilibrium will not point straight down, the condition of symmetry on the inertia tensor will not be satisfied and therefore we will not have extended Rosenberg modes.

We start by computing the generators of the quintuple pendulum up to an energy level of $E_{max} = 100\text{J}$. Unfortunately, the visualization in five-dimensional configuration space becomes rather complicated. Therefore, we will first show a few projections and then look at motions in Cartesian space. The lower triangular matrix in Fig. 8 shows the computed generators in mutual projection onto the q_iq_j-planes. Then, for each generator, we select the configuration of maximal energy, which is indicated by the dots in the figure. We take these configurations as initial configuration and simulate the pendulum. This will result in a periodic trajectory in form of a modal oscillation. The projected trajectory is shown in the upper triangular matrix in Fig. 8. All the oscillation pass, as predicted by Theorem 1 through the equilibrium in the center.

To achieve a better intuition on how the pendulum behaves we also show the generators and highest energy modal oscillation in Fig. 9. The equilibrium configuration of the pendulum is reached when all links are pointing straight downwards. All the modal oscillation pass through that configuration. So far we have only shown the highest energy modal oscillation. However, the modal oscillation for all energy levels pass through the equilibrium. Let us select, for instance, the fourth generator and look at modal oscillations for various energy levels in Fig. 10. The left pane shows the initial configuration of the pendulum, while the right pane

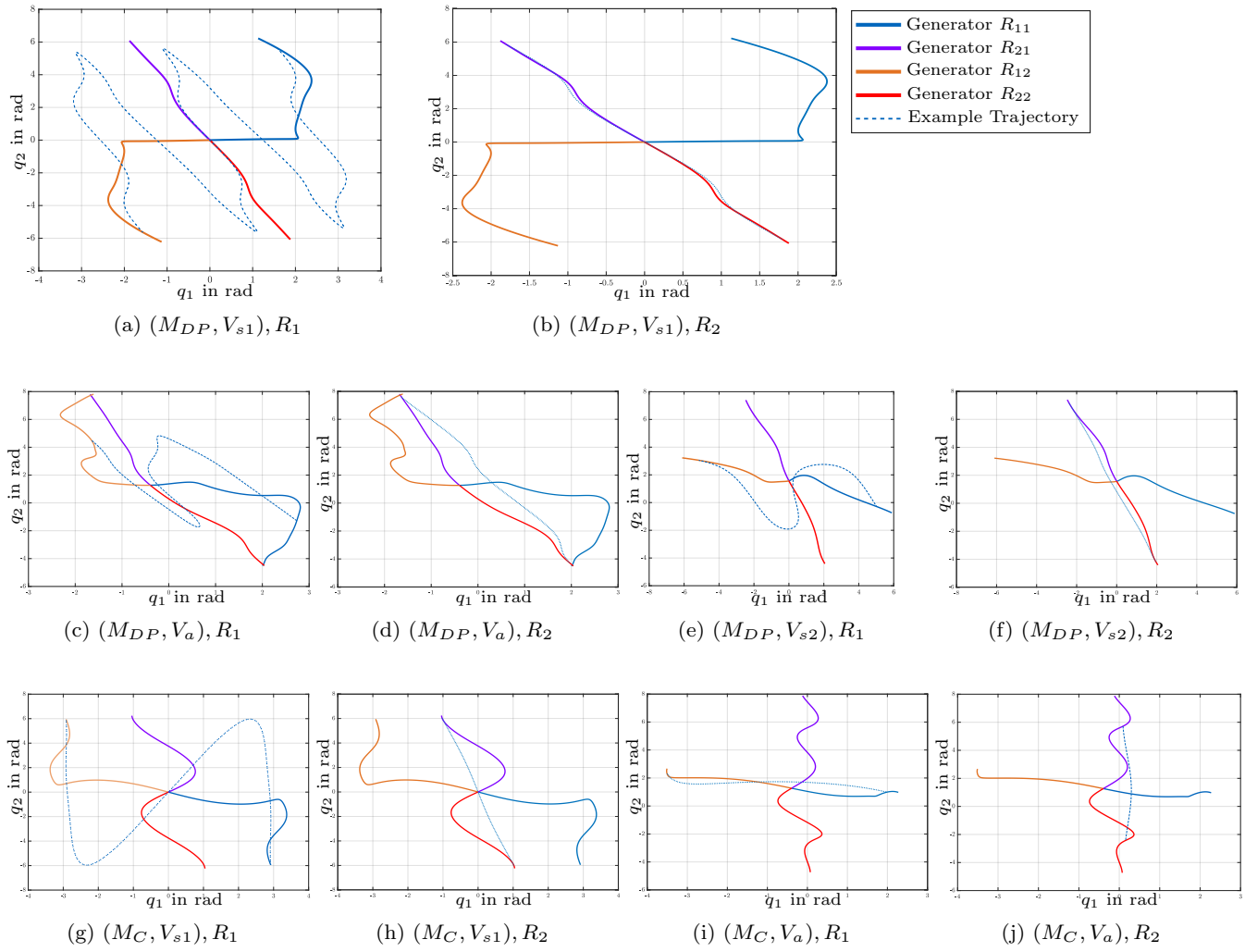

(a) $(M_{DP}, V_{s1}), R_1$ (b) $(M_{DP}, V_{s1}), R_2$

(c) $(M_{DP}, V_a), R_1$ (d) $(M_{DP}, V_a), R_2$ (e) $(M_{DP}, V_{s2}), R_1$ (f) $(M_{DP}, V_{s2}), R_2$

(g) $(M_C, V_{s1}), R_1$ (h) $(M_C, V_{s1}), R_2$ (i) $(M_C, V_a), R_1$ (j) $(M_C, V_a), R_2$

Fig. 5: Results of numerical continuation for different example systems generated by combining different potential functions and inertia tensors. The solid lines show computed generators of the system. The pair of blue and orange solid lines show the two generators associated to the first eigenmanifold and the pair of purple and red the two associated to the second eigenmanifold. The dashed blue line shows an example modal oscillation of the system for one energy. The conditions states by Theorem 1 are satisfied for the cases (a,b) and (g,h).

shows the trajectories of the point masses. Again, we observe that all modal oscillation pass through a configuration where all links point straight downwards.

present a more suitable definition to identify nonlinear normal modes in conservative nonlinear systems than extended Rosenberg modes do.

6 Conclusion

In this paper, we presented a sufficient condition that follows from symmetries of the system (1) and explains the presence of continuous families of extended Rosenberg modes in a general conservative scenario. The absence of such continuous families was observed when these conditions were violated, which suggests that they are not very common. At the same time, the Eigenmanifolds defined by Albu-Schäffer and Della Santina [3] still exists for these systems. This indicates that they

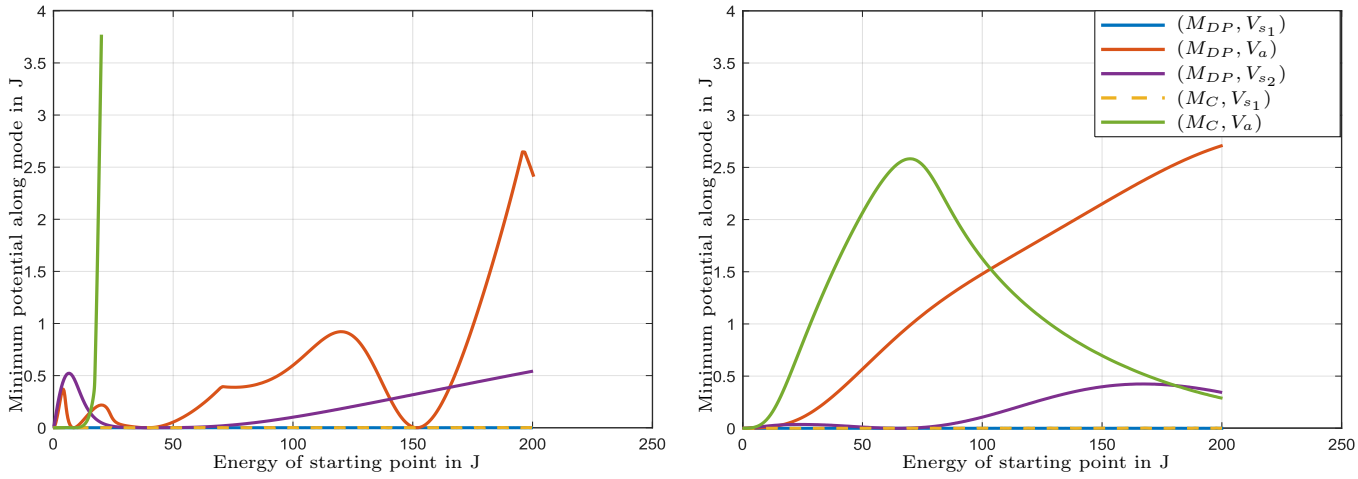

(a) Generators R_1 (b) Generators R_2

Fig. 6: Minimal potential energy for modes of the example systems, split by modes collected on first and second generator.

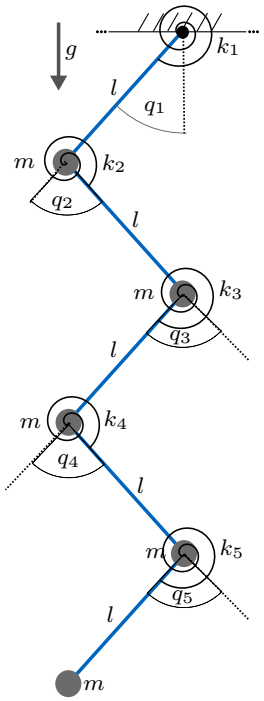

Fig. 7: Quintuple Elastic Pendulum in Gravity Field

7 Appendix: Coordinate-free Perspective

From a differential geometric perspective Hamiltonian systems are described on symplectic manifolds (M, ω), which consist of a $2n$-dimensional manifold M and a closed, non-degenerate 2-form ω called the symplectic form.
Given a configuration space Q and a cotangent bundle T^*Q, the Hamiltonian systems considered in this work are described on symplectic manifolds (T^*Q, ω) with ω the canonical symplectic form that reads

$$\omega = dp^i \wedge dq_i \tag{33}$$

in any system of coordinates $(q_1, ..., q_n)$ on Q and fibre-wise coordinates $(p_1, ..., p_n)$ with respect to the cotangent basis $(dq_1, ..., dq_n)$. The Hamiltonian $H : T^*Q \to \mathbb{R}$ is then given as the sum of a bi-linear, symmetric kinetic energy $K_{\mathcal{Q}} : T^*_{\mathcal{Q}}Q \times T^*_{\mathcal{Q}}Q \to \mathbb{R}$ and a potential energy $V : Q \to \mathbb{R}$

$$H(\mathcal{Q}, \mathcal{P}) = K_{\mathcal{Q}}(\mathcal{P}, \mathcal{P}) + V(\mathcal{Q}) \,. \tag{34}$$

Through the symplectic form ω, the gradient dH of this Hamiltonian, which is a co-vector field, is then uniquely associated with a vector field X_H, whose integral curves determine the evolution of the Hamiltonian system. X_H is defined implicitly, as the vector field that satisfies, for any vector field Y:

$$dH(Y) = \omega(X_H, Y) \,. \tag{35}$$

Integral curves are defined as $\gamma : \mathbb{R} \to T^*Q$ that satisfy

$$\dot{\gamma} = X_H \,. \tag{36}$$

Symmetries are then diffeomorphisms $S : T^*Q \to T^*Q$ that map integral curves $\gamma : \mathbb{R} \to T^*Q$ into other integral curves. That is, they satisfy

$$\tau S_* X_H = X_{H \circ S} \tag{37}$$

for $\tau \in \mathbb{R}$. Here, $S_* : TT^*Q \to TT^*Q$ denotes the push-forwad of S. If such an S and τ can be found, then it is guaranteed that for $\gamma_1(t)$ an integral curve of X_H, $\gamma_2(t) = S(\gamma_1(\tau t)$ is also an integral curve of X_H. This

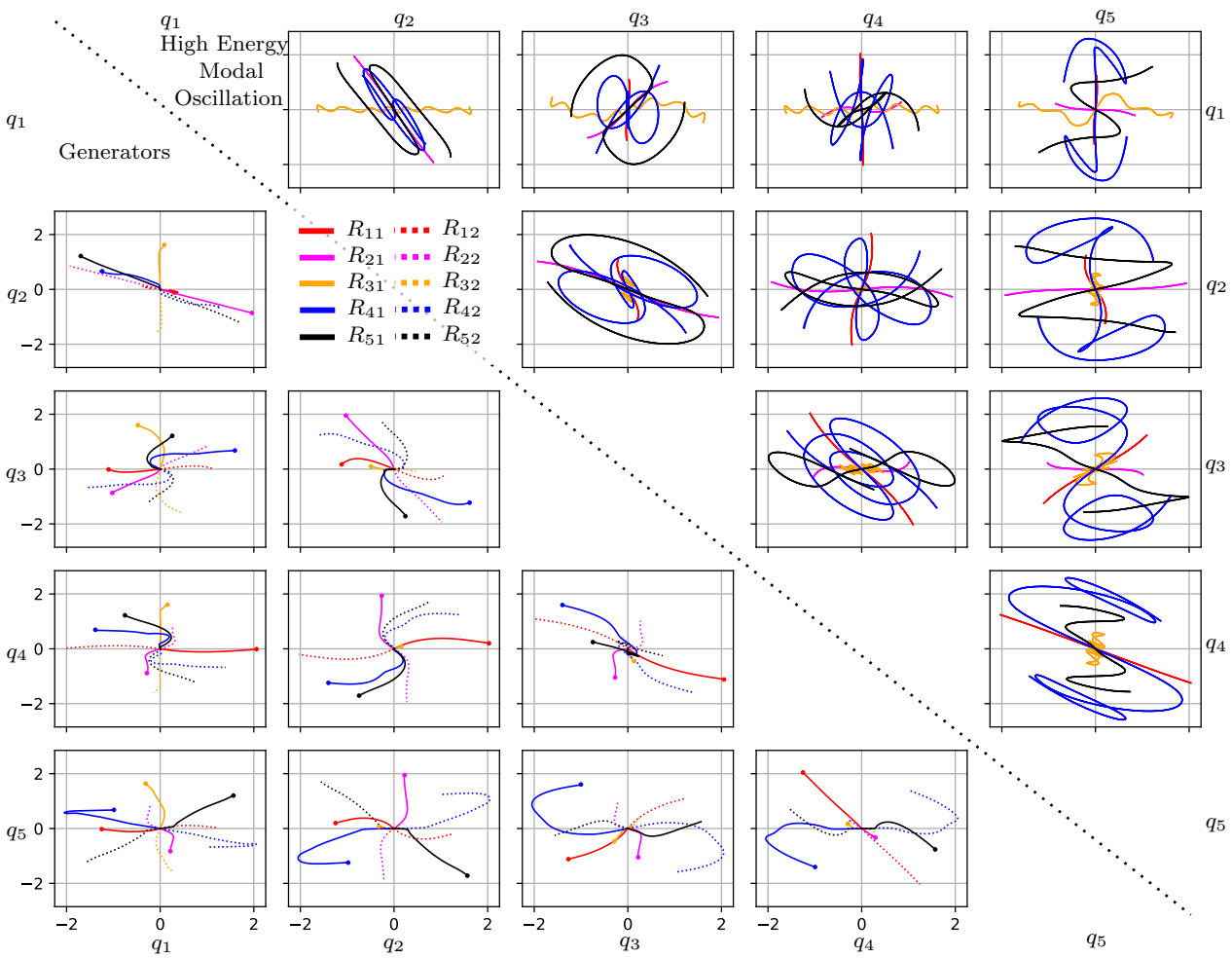

Fig. 8: Generators and high energy modal oscillations of the quintuple pendulum shown in configuration space. The lower triangular matrix of plots shows the generators projected onto different q_iq_j-planes. The upper triangular matrix of plots shows the corresponding modal oscillation for the highest energy on the color-matching generator. As the quintuple pendulum satisfies Theorem 1 all modal oscillations pass through the equilibrium. This is only shown for the highest energy oscillation, but the same is true for every other energy level.

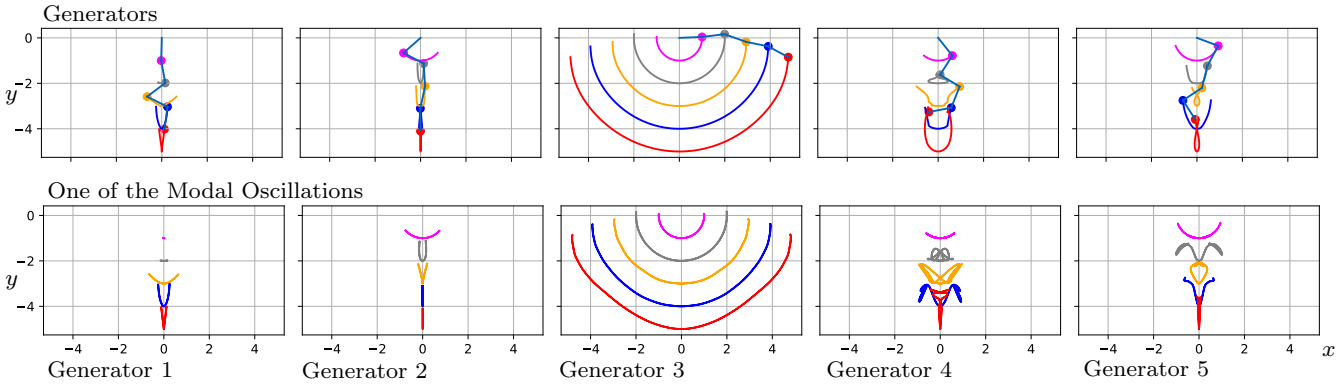

Fig. 9: Cartesian version of Fig. 8. The top row shows the generators as Cartesian paths of the joints and the bottom row shows one modal oscillation. All of the modal oscillation pass through the equilibrium where all of the links of the pendulum point straight down.

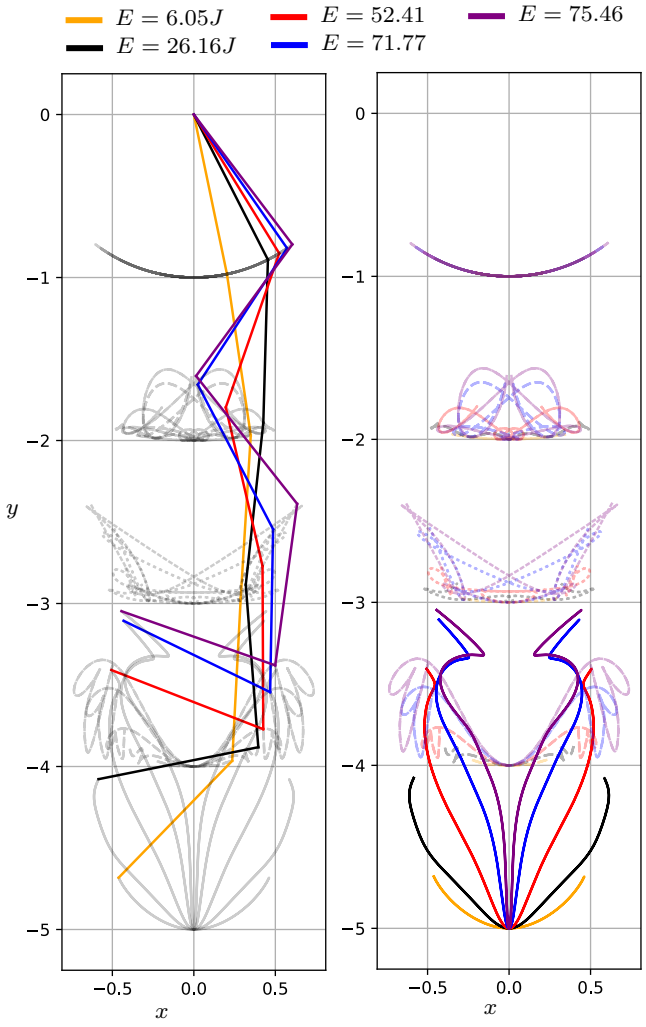

Fig. 10: Modes with different energy levels for the fourth eigenmanifold. The engeinmanifold is of the extended Rosenberg type. On the left the initial configurations are shown. On the right the modal oscillations of the tip are visualized in Cartesian space.

can be verified by writing out the tangent vector of $S(\gamma_1(\tau t))$.

This article then investigates the presence of two particular symmetries $S_1 = (id_Q, -id_{T_q^*Q})$ with $\tau_1 = -1$ and $S_2 = (R, (R^{-1})^*)$ with $\tau = 1$ and $R : Q \to Q$ a diffeomorphism with $\bar{q} \in Q$ the only fixed point of the transformation, and $(R^{-1})^*$ denotes the pullback of its inverse.

The presence of such symmetries has to be verified in coordinates, but this differential geometric picture shows the coordinate independent nature of such a verification. The consequences of these symmetries can then also be analyzed in a coordinate-free scenario. Given that (S_1, τ_1) satisfy (37), a fixed point of the transformation S_1 results in two solutions $\gamma_1(t)$ and $\gamma_2(t) = S_1(\gamma_1(\tau_1 t))$, and by uniqueness of solutions it then follows that

$$\gamma(t) = S_1(\gamma(-t)) \quad \text{if} \quad \gamma(0) = S_1(\gamma(0))\,. \tag{38}$$

This would give rise to Lemmas 1 and 2, with analogous proofs.

Given that (S_2, τ_2) satisfy (37) and $S_2 = (R, (R^{-1})^*)$, where R has a unique fixed point $\bar{q}$, then S_2 has the unique fixed point $(\bar{q}, 0)$. The presence of this symmetry roughly means that any global structure that depends on the local flow X_H should also be symmetric about this point. Again, uniqueness of solutions would yield

$$\gamma(t) = S_2(\gamma(t + T/2)) \quad \text{if} \quad \gamma(0) = S_2(\gamma(0))\,, \tag{39}$$

which gives rise to Lemmas 3 and 4, with likewise analogous proofs.

Finally, Theorem 1 would follow by requiring that both (S_1, τ_1) and (S_2, τ_2) satisfy (37), together with requiring unicity of the generators.

Data Statement

The datasets generated during and/or analysed during the current study are available from the corresponding author on reasonable request.

Conflicts of Interest

The authors declare that they have no conflict of interest.

Funding

This work is supported by EU Project 835284 M-Runners.

References

1. R. Rosenberg, "On nonlinear vibrations of systems with many degrees of freedom," in *Advances in Applied Mechanics* (G. Chernyi, H. Dryden, P. Germain, L. Howarth, W. Olszak, W. Prager, R. Probstein, and H. Ziegler, eds.), vol. 9 of *Advances in Applied Mechanics*, pp. 155 – 242, Elsevier, 1966.
2. M. Peeters, R. Viguié, G. Sérandour, G. Kerschen, and J. C. Golinval, "Nonlinear normal modes, Part II: Toward a practical computation using numerical continuation techniques," *Mechanical Systems and Signal Processing*, vol. 23, pp. 195–216, Jan. 2009.
3. A. Albu-Schäffer and C. Della Santina, "A review on nonlinear modes in conservative mechanical systems," *Annual Reviews in Control*, vol. 50, pp. 49 – 71, 2020.
4. R. Featherstone, *Rigid body dynamics algorithms*. Springer, 2014.

5. F. C. Park, B. Kim, C. Jang, and J. Hong, "Geometric algorithms for robot dynamics: A tutorial review," *Applied Mechanics Reviews*, vol. 70, no. 1, 2018.
6. A. Seth, J. L. Hicks, T. K. Uchida, A. Habib, C. L. Dembia, J. J. Dunne, C. F. Ong, M. S. DeMers, A. Rajagopal, M. Millard, *et al.*, "Opensim: Simulating musculoskeletal dynamics and neuromuscular control to study human and animal movement," *PLoS computational biology*, vol. 14, no. 7, p. e1006223, 2018.
7. A. Di Russo, D. Stanev, S. Armand, and A. Ijspeert, "Sensory modulation of gait characteristics in human locomotion: A neuromusculoskeletal modeling study," *PLOS Computational Biology*, vol. 17, no. 5, p. e1008594, 2021.
8. L. Renson, G. Kerschen, and B. Cochelin, "Numerical computation of nonlinear normal modes in mechanical engineering," *Journal of Sound and Vibration*, vol. 364, pp. 177–206, Mar. 2016.
9. D. A. Ehrhardt, T. L. Hill, and S. A. Neild, "Experimentally measuring an isolated branch of Nonlinear normal modes," *Journal of Sound and Vibration*, vol. 457, pp. 213–226, Sept. 2019.
10. K. V. Avramov and Y. V. Mikhlin, "Review of Applications of Nonlinear Normal Modes for Vibrating Mechanical Systems," *Applied Mechanics Reviews*, vol. 65, Apr. 2013.
11. S. W. Shaw and C. Pierre, "Normal Modes for Non-Linear Vibratory Systems," *Journal of Sound and Vibration*, vol. 164, pp. 85–124, June 1993.
12. A. F. Vakakis and R. H. Rand, "Normal modes and global dynamics of a two-degree-of-freedom non-linear system - I. Low energies," *International Journal of Non-Linear Mechanics*, vol. 27, pp. 861–874, Sept. 1992.
13. I. Kovacic, M. Zukovic, and D. Radomirovic, "Normal modes of a double pendulum at low energy levels," *Nonlinear Dynamics*, vol. 99, no. 3, pp. 1893–1908, 2020.
14. C. Della Santina and A. Albu-Schäffer, "Exciting Efficient Oscillations in Nonlinear Mechanical Systems Through Eigenmanifold Stabilization," *IEEE Control Systems Letters*, vol. 5, pp. 1916–1921, Dec. 2021.
15. C. Della Santina, D. Calzolari, A. M. Giordano, and A. Albu-Schäffer, "Actuating Eigenmanifolds of Conservative Mechanical Systems via Bounded or Impulsive Control Actions," *IEEE Robotics and Automation Letters*, vol. 6, pp. 2783–2790, Apr. 2021.
16. F. Bjelonic, A. Sachtler, A. Albu-Schaffer, and C. Della Santina, "Experimental closed-loop excitation of nonlinear normal modes on an elastic industrial robot," *IEEE Robotics and Automation Letters*, 2022.
17. J. Moyrón, J. Moreno-Valenzuela, and J. Sandoval, "Orbital stabilization for linear mechanical systems via a speed gradient algorithm," in *2021 26th International Conference on Automation and Computing (ICAC)*, pp. 1–5, IEEE, 2021.
18. J. G. Romero and B. Yi, "Orbital stabilization of underactuated mechanical systems without euler-lagrange structure after of a collocated pre-feedback," *arXiv preprint arXiv:2109.06724*, 2021.
19. C. F. Sætre, A. S. Shiriaev, L. B. Freidovich, S. V. Gusev, and L. M. Fridman, "Robust orbital stabilization: A floquet theory–based approach," *International Journal of Robust and Nonlinear Control*, vol. 31, no. 16, pp. 8075–8108, 2021.
20. G. Garofalo and C. Ott, "Passive energy-based control via energy tanks and release valve for limit cycle and compliance control," *IFAC-PapersOnLine*, vol. 51, no. 22, pp. 73–78, 2018.
21. Z. Gan, Y. Yesilevskiy, P. Zaytsev, and C. D. Remy, "All common bipedal gaits emerge from a single passive model," *Journal of The Royal Society Interface*, vol. 15, no. 146, p. 20180455, 2018.
22. N. Kashiri, A. Abate, S. J. Abram, A. Albu-Schaffer, P. J. Clary, M. Daley, S. Faraji, R. Furnemont, M. Garabini, H. Geyer, *et al.*, "An overview on principles for energy efficient robot locomotion," *Frontiers in Robotics and AI*, vol. 5, p. 129, 2018.
23. R. Balderas Hill, S. Briot, A. Chriette, and P. Martinet, "Performing energy-efficient pick-and-place motions for high-speed robots by using variable stiffness springs," *Journal of Mechanisms and Robotics*, pp. 1–12, 2021.
24. R. L. Hatton, Z. Brock, S. Chen, H. Choset, H. Faraji, R. Fu, N. Justus, and S. Ramasamy, "The geometry of optimal gaits for inertia-dominated kinematic systems," *arXiv preprint arXiv:2102.01506*, 2021.
25. A. Seyfarth, "Template-based approach to resolve redundancies in motor control," in *Novel Bioinspired Actuator Designs for Robotics*, pp. 21–25, Springer, 2021.
26. A. A. Biewener, R. J. Bomphrey, M. A. Daley, and A. J. Ijspeert, "Stability and manoeuvrability in animal movement: lessons from biology, modelling and robotics," 2022.
27. M. Baake, "A Brief Guide to Reversing and Extended Symmetries of Dynamical Systems," in *Ergodic Theory and Dynamical Systems in their Interactions with Arithmetics and Combinatorics* (S. Ferenczi, J. Kułaga-Przymus, and M. Lemańczyk, eds.), Lecture Notes in Mathematics, pp. 117–135, Cham: Springer International Publishing, 2018.
28. N. Román-Roy, "A summary on symmetries and conserved quantities of autonomous Hamiltonian systems," *Journal of Geometric Mechanics*, vol. 12, no. 3, p. 541, 2020.
29. V. A. Abakumova, D. S. Kaparulin, and S. L. Lyakhovich, "Multi-Hamiltonian formulations and stability of higher-derivative extensions of $3d$ Chern-Simons," *Eur.Phys.J.C*, vol. 78, no. 2, p. 115, 2018.
30. F. X. Mei, H. B. Wu, and Y. F. Zhang, "Symmetries and conserved quantities of constrained mechanical systems," *International Journal of Dynamics and Control*, vol. 2, pp. 285–303, Sept. 2014.
31. J. Butterfield, *Physical Theory and its Interpretation: Essays in Honor of Jeffrey Bub*, ch. On Symmetry and Conserved Quantities in Classical Mechanics, pp. 43–100. Dordrecht: Springer Netherlands, 2006.
32. R. Alomair and J. Montaldi, "Periodic Orbits in Hamiltonian Systems with Involutory Symmetries," *Journal of Dynamics and Differential Equations*, vol. 29, pp. 1283–1307, Dec. 2017.
33. G. M. Chechin, V. P. Sakhnenko, H. T. Stokes, A. D. Smith, and D. M. Hatch, "Non-linear normal modes for systems with discrete symmetry," *International Journal of Non-Linear Mechanics*, vol. 35, pp. 497–513, May 2000.
34. G. Russo and J.-J. E. Slotine, "Symmetries, stability, and control in nonlinear systems and networks," *Physical Review E*, vol. 84, p. 041929, Oct. 2011.
35. S. Ozana, T. Docekal, A. Kawala-Sterniuk, J. Mozaryn, M. Schlegel, and A. Raj, "Trajectory Planning for Mechanical Systems Based on Time-Reversal Symmetry," *Symmetry*, vol. 12, p. 792, May 2020.
36. F. Bullo and A. D. Lewis, *Geometric Control of Mechanical Systems*, vol. 49 of *Texts in Applied Mathematics*. New York-Heidelberg-Berlin: Springer Science+Business Media New York, 2004.

37. V. Záda and K. Belda, "Mathematical modeling of industrial robots based on Hamiltonian mechanics," in *International Carpathian Control Conference (ICCC)*, vol. 17, pp. 813–818, May 2016.
38. J. S. W. Lamb and J. A. G. Roberts, "Time-reversal symmetry in dynamical systems: A survey," *Physica D: Nonlinear Phenomena*, vol. 112, pp. 1–39, Jan. 1998.